small

Thermal Modulation of Nanomotor Movement

Shankar Balasubramanian, Daniel Kagan, Kalayil Manian Manesh, Percy Calvo-Marzal, Gerd-Uwe Flechsig, and Joseph Wang**

Motion control is essential for various applications of man-made nanomachines. The ability to control and regulate the movement of catalytic nanowire motors is illustrated by applying short heat pulses that allow the motors to be accelerated or slowed down. The accelerated motion observed during the heat pulses is attributed primarily to the thermal activation of the redox reactions of the H_2O_2 fuel at the Pt and Au segments and to the decreased viscosity of the aqueous medium at elevated temperatures. The thermally modulated motion during repetitive temperature on/off cycles is highly reversible and fast, with speeds of 14 and 45 $\mu m\ s^{-1}$ at 25 and 65 °C, respectively. A wide range of speeds can be generated by tailoring the temperature to yield a linear speed–temperature dependence. Through the use of nickel-containing nanomotors, the ability to combine the thermally regulated motion of catalytic nanomotors with magnetic guidance is also demonstrated. Such on-demand control of the movement of nanowire motors holds great promise for complex operations of future manmade nanomachines and for creating more sophisticated nanomotors.

Keywords:
- catalytic nanowires
- nanomachines
- nanomotors
- hydrogen peroxide
- temperature modulation

1. Introduction

There has been considerable interest in the development of artificial nanomachines based on catalytic nanowire motors.[1] Such manmade nanomotors rely on the propulsion of asymmetric (bisegment) nanowires in the presence of a chemical fuel (commonly H_2O_2). While various mechanisms have been proposed for the self-propulsion of bimetallic catalytic nanomotors, the most accepted ones rely on electrokinetic self-electrophoresis and oxygen bubble formation. Both of these mechanisms are associated with the electrocatalytic decomposition of the peroxide fuel. The autonomous motion of these chemically powered nanomachines holds great promise for a wide range of future applications, from nanoscale transport and distribution to nanosurgical operations. Recent advances have illustrated significant improvements in the speed and power of catalytic nanomotors through judicious control of the nanowire or fuel composition.[2,3] Precise motion control is another important feature and challenge of synthetic nanomotors. Regulating on-demand the movement of nanomotors is essential for different future applications. Magnetically directed movement of nanowire motors was accomplished through the incorporation of a ferromagnetic (nickel) segment.[4] This allowed for magnetic guidance and steering in the presence of an external magnetic field,[4] as well as a ''stop-and-go'' operation through a modulated magnetic field.[2] Such a response to changes in the local environment holds great promise for controlling the operation of artificial functional nanomotors.

Here we demonstrate how temperature-modulated motion of catalytic nanomotors can be achieved by applying short heat pulses. Temperature-dependent electrochemical processes have received considerable recent attention in connection with hot-wire electrochemistry as recent reviews have pointed out.[5] This technique involves the use of electrically heated electrodes for enhanced electrochemical measurements

[*] Prof. J. Wang, Dr. S. Balasubramanian, D. Kagan, Dr. K. M. Manesh, Dr. P. Calvo-Marzal
Department of Nanoengineering
University of California, San Diego
La Jolla, CA 92093 (USA)
E-mail: josephwang@ucsd.edu
Dr. G.-U. Flechsig
University of Rostock, Department of Chemistry
D-18051 Rostock (Germany)
E-mail: gerd-uwe.flechsig@uni-rostock.de

Supporting Information is available on the WWW under http://www.small-journal.com or from the author.

DOI: 10.1002/smll.200900023

© 2009 Wiley-VCH Verlag GmbH & Co. KGaA, Weinheim

through accelerated kinetics of redox processes and/or increased rates of mass transport. In the following sections, we will illustrate an analogous high-temperature propulsion of catalytic nanomotors and the use of heat pulses for regulating on demand the motion of these nanowire motors. Unlike hot-wire electrochemistry where the wire serves as the heated working electrode, the heated wire acts here solely as the heat source for controlling the solution temperature in the plane of the nanomotors (see Supporting Information, Figure S1). The use of heat pulses leads to a thermal modulation of the movement of artificial nanomotors with a fine, reversible and rapid control of the nanomotor velocity. Finally, we will illustrate the coupling of the new thermally regulated motion with magnetic guidance towards a more advanced temporal and spatial motion control.

2. Results and Discussion

2.1. On-Demand Reversible Thermal Modulation of the Nanomotor Movement

Figure 1 illustrates the accelerated velocity of catalytic nanomotors associated with the high-temperature electrochemical propulsion. It compares traces of three Au–Pt nanomotors, taken from videos of the nanowires in the presence of the peroxide fuel using room temperature (A) and elevated temperature (B) over a 2 s period. The heat source (a 25-μm-diameter Au-coated Pt wire) was placed 30 μm above the plane of the nanomotors (see Supporting Information, Figure S1), leading to a temperature of 65 °C in that plane (in connection to a DC heat current of 600 mA).[6,7] The nanowires exposed to the elevated temperature travel substantially (≈3 fold) longer distances than the "room-temperature" motors over the same time period (average distance of 90 versus 28 μm). Such distances correspond to speeds of 45 and 14 μm s^{-1} for the elevated and room temperatures, respectively. Videos illustrating such high-temperature and room-temperature electrochemical propulsions are shown in the Supporting Information (Video 1). The increased speed is attributed to the accelerated kinetics of the redox reactions of the peroxide fuel (on both segments) and to a lower solution viscosity (and hence diminished friction forces) with the rising temperature (see discussion below). In view of a microscale convection around hot-wire electrodes,[6–8] a control experiment, performed without the peroxide fuel, examined potentially disturbing convective effects at the elevated temperature. This revealed almost no self-propelled non-Brownian motion, with only a slight drift due to a weak thermal convection (3 μm s^{-1}; not shown). Apparently, the self-propelled nanomotors are not prone to convection effect (in presence of the fuel) provided that they are kept on the surface of the microscopic glass slide (placed at a distance larger than 20 μm from the heat source).

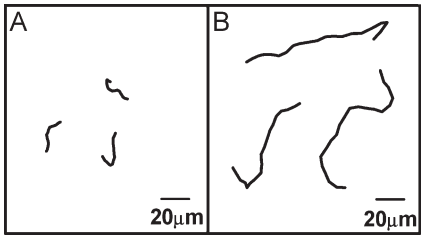

Figure 1. High-temperature electrochemical propulsion. Tracking lines of nanomotors illustrating the distances traveled by three Au–Pt nanowires at room temperature (A) and at an elevated temperature of 65 °C (B) using a 5 wt% H_2O_2 fuel solution. The elevated temperature was obtained by using a heating current of 600 mA with the Au-coated Pt wire located 30 μm above the plane of the nanomotors. The temperature refers to the focal plane of the nanomotors.

The high-temperature electrochemical propulsion offers a fine and reversible control over the nanomotor velocity. Figure 2 examines the influence of different temperature pulse amplitudes upon the nanomotor speed in a 5 wt% peroxide solution. It displays speed–time profiles for 3 s temperature pulses to 40 (a), 48 (b), and 58 °C (c) (in the plane of the observed nanomotors). In all three cases, the speed increases rapidly with the time at first, leveling off towards the end of the pulse, and reaching maximal values of 25, 31, and 38 μm s^{-1} at 40, 48, and 58 °C, respectively. Similarly, a sharp decrease in the velocity is observed upon switching the heat off, approaching the original ("cold") value within 10 s. Such speed profiles reflect the temporal heat formation and cooling down process during the heat pulse and are consistent with earlier temperature profiles during short heat pulses (also at 25-μm-diameter Pt wire).[8] The spread of heat in the solution surrounding the hot wires and the corresponding temperature profiles have been calculated numerically.[6,7] For example, an 80 °C wire surface temperature corresponds to a solution temperature of 50 °C at a 40-μm distance below the wire center.[6] Different solution temperatures (at the nanomotor plane) have been estimated in a similar fashion for different

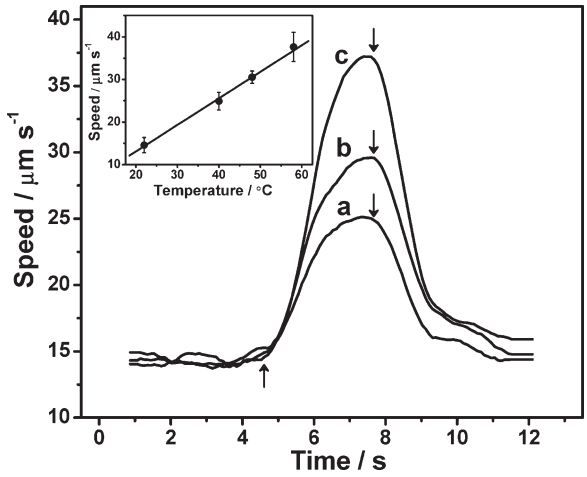

Figure 2. Speed–time profiles of Au–Pt nanomotors during different 3 s heat pulses to 40 (a), 48 (b), and 58 °C (c) in a 5 wt% H_2O_2 solution. The arrows (around 5 and 8 s) correspond to the time of switching the heating current on and off, respectively. Data shown represent the average speed of 60 nanomotors. Raw data have been smoothed using fast Fourier transformation (Origin software; 5 points). Inset displays the linear relationship between the nanomotor speed and the temperature. Temperatures refer to the focal plane of the nanomotors. The error bars correspond to standard deviations, calculated on the basis of 4 nanomotor tracks.

 © 2009 Wiley-VCH Verlag GmbH & Co. KGaA, Weinheim

heating currents and source–plane distances for both Pt and Au wires (see Supporting Information, Figure S2a and b). The data of Figure 2 indicate that a wide range of nanomotor speeds can be generated through a fine control of the temperature. Indeed, the inset of Figure 2 illustrates a linear relation between the temperature and the nanomotor speed over the 14 to 37 $\mu m\ s^{-1}$ range (slope: 0.635 $\mu m\ s^{-1}\ {}^{\circ}C^{-1}$). Such a linear relation between the temperature and the nanomotor speed is somewhat surprising in view of the complex temperature-dependent processes and opposing thermal effects (discussed below).

The speed–temperature profiles of Figure 2 indicate great promise for regulating on-demand the motion of catalytic nanowire motors in connection to an external on/off temperature switch. A video illustrating the thermally modulated speed during a heat pulse to 50 °C is shown in the Supporting Information (Video 2). A dramatic speed acceleration from 11 to 37 $\mu m\ s^{-1}$ and deceleration to 12 $\mu m\ s^{-1}$ are observed during this 4 s temperature pulse. The ability to thermally modulate the motion of catalytic nanomotors is also illustrated using the five short heat pulses of Figure 3. Reversible changes in the speed of the Pt–Au nanomotor (between 17 and 28 $\mu m\ s^{-1}$) are observed during these repetitive heating and cooling periods. Note that due to the short duration of the heat pulse (1.5 s), the nanomotors do not reach their maximal steady-state speed value. Depending on the heating current, it takes up to 2 s for the system to reach a thermal steady state.[8] Therefore, temperatures lower than the steady-state value are expected using the short heat pulses of Figure 3 compared to long pulses (e.g., Figure 2) or use of continuous heating (e.g., Figure 1B). This modulated motion can be repeated continuously and reversibly, indicating negligible fuel depletion in the plane of the nanomotors (as expected from the small voltage drop along the heated wire and its distance to the nanomotor plane). Similar switching of the movement of biological motors has been reported, including a temperature-induced acceleration of the biomotor actomyosin[9] and a light-induced modulated speed of kinesin in connection to the controlled release of its ATP fuel.[10] It should be noted that these biomotors respond slowly (within a few minutes) to these external stimuli, as compared to the instantaneous (seconds) thermal "switching" of the present synthetic nanomotor system.

Directed motion of the thermally stimulated nanomotors (essential for diverse applications) has been accomplished by incorporating a ferromagnetic nickel segment and aligning the magnetized nanowires using an external magnetic field. Figure 4a demonstrates the ability to combine the thermally regulated motion of catalytic nanomotors with magnetic guidance. It depicts the speed modulation during two 3 s heat pulses to 50 °C (gray lines) while aligning the Au–Ni–Pt nanowire in a relatively straight line under a weak magnetic field. The dramatic speed acceleration during the heat pulses is indicated from the 2.5-fold larger displacement of the nanomotor (versus the path observed during the intermittent 3 s "cooling" period; black, bold line). The slight deviation from the straight line during the pulses reflects the negligible thermal convective drift (discussed earlier). The corresponding temperature–time profile (shown on the top, Figure 4b) indicates that the speed increases rapidly upon applying the heat pulse, reaching a maximal value of 25 $\mu m\ s^{-1}$, and decreases sharply back to 10 $\mu m\ s^{-1}$ during the cooling period. Similarly, it would be possible to combine the accelerated motion with magnetic steering at different directions at preselected locations and times, as well as with a magnetic loading and unloading of cargo. Coupling of magnetic guidance with an on-demand thermal motion control leads to a more advanced (spatial and temporal) motion control and holds great promise for performing demanding tasks and creating more sophisticated nanomotors.

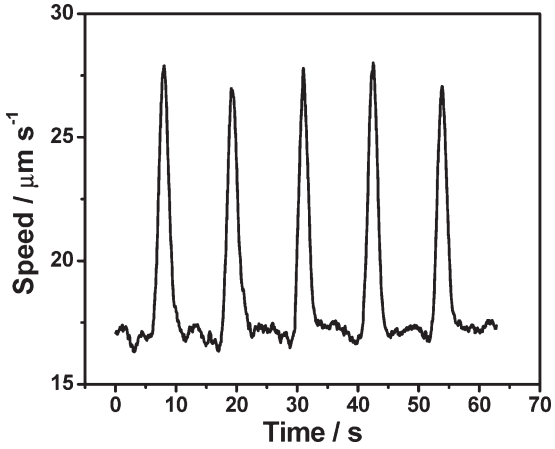

Figure 3. Modulated motion of catalytic nanomotors during five 1.5 s heat pulses (corresponding to a temperature of 50 °C) at 11.5 s intervals. Data shown represent the average speed of 3 nanomotors. The elevated temperature was obtained by using a heat current of 700 mA with the Au wire located 35 μm above the plane of the nanomotors. Data processing as in Figure 2.

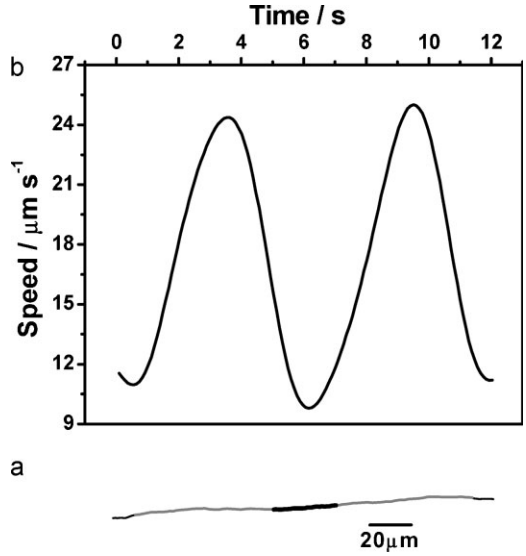

Figure 4. High-temperature propulsion of magnetically guided Ni-containing nanomotor. Shown (a, bottom) is the path during two 3 s heat pulses (gray) with an intermittent off period of 3 s (black, bold). Au heating wire (25-μm-diameter) placed at 30-μm distance from the plane of the nanomotors. Also shown (b, top) is the corresponding speed–time profile. Data processing as in Figure 2.

© 2009 Wiley-VCH Verlag GmbH & Co. KGaA, Weinheim

2.2. Temperature Effect upon the Kinetics of Electrochemical Processes of the Fuel

Tafel plots were used to examine the thermal activation of the electrochemical processes of the peroxide fuel at the Pt and Au segment materials and temperature-induced changes in the mixed potential difference (ΔE) of the fuel at the corresponding materials. Figure 5 depicts plots for the H_2O_2 reaction at Pt and Au disk electrodes using solution temperatures of 25, 40, and 60 °C. Gradual potential shifts from 181 to 171 mV (Pt) and from 236 to 258 mV (Au) are observed upon raising the temperature from 25 to 60 °C. Such plots indicate a thermally induced accelerated kinetics of both the oxidation and reduction reactions of the peroxide fuel. This thermal activation is also indicated from the increased current densities (at both electrodes) upon raising the temperature. The larger potential shift observed at the Au electrode indicates that the temperature effect is more pronounced for the cathodic reaction at this material. This is consistent with the larger temperature-induced acceleration of reaction processes with higher activation energy.[8,11–13] The self-electrophoresis mechanism of asymmetric nanowire motors suggests that the speed of the nanomotors is proportional to the mixed potential difference (ΔE) of the fuel at the corresponding segment materials.[14] Indeed, the opposite potential shifts observed at the Pt and Au electrodes upon raising the temperature lead to larger ΔE values of 66 and 87 mV (at 40 and 60 °C, respectively), compared to the 54 mV value of the room temperature (Figure 5). This increase of the ΔE value with the temperature is consistent with the speed–temperature profile of Figure 2. The oxygen bubble formation propulsion mechanism, which also involves the electrochemical decomposition of the fuel, can also explain the observed nanomotor acceleration on the basis of such temperature-induced activation of the electrochemical fuel reactions.

While Figure 5 indicates that the accelerated motion observed at elevated temperatures reflects the thermal activation of the electrochemical reactions of the H_2O_2 fuel, one should consider other thermal effects influencing the nanomotor movement. In particular, the dynamic viscosity (μ) of water decreases in a nonlinear manner by ≈50% upon increasing the temperature from 20 to 55 °C[15] and this is expected to double the velocity v of the nanomotor (assuming that F_D, the frictional force in Stokes law, is constant). In practice, the propulsion force F_P (same value, opposite direction compared to F_D) should also increase with the temperature due to the accelerated reaction kinetics at the nanomotor surface. In contrast, raising the temperature increases the solution conductivity as well as the autoprotolysis of water, and these changes are expected to decrease the nanomotor speed. While some of the above thermal effects compensate each other, the net result is a dramatic enhancement of the nanomotor motion upon applying the heat pulses, and a (somewhat surprising and coincidental) linear dependence between the speed and the temperature (Figure 2, inset).

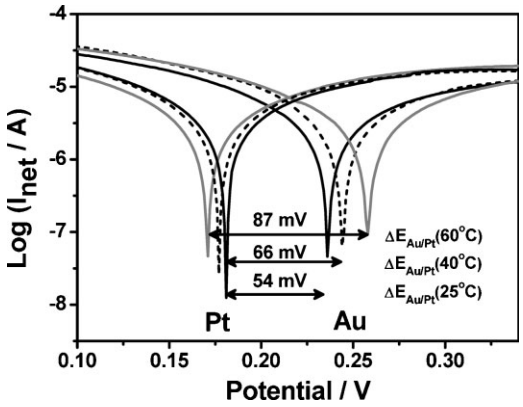

Figure 5. Tafel plots at Pt and Au disk electrodes in a 5 wt% H_2O_2 solution at different temperatures. The mixed potential differences (ΔE, Pt versus Au) are also indicated in the figure.
Reference electrode: Ag/AgCl (3 M NaCl).

3. Conclusions

In conclusion, we demonstrated a novel approach for modulating and thermally activating the motion of catalytic nanomotors. This reversible thermal control represents a novel approach for regulating on-demand the operation of artificial nanomotors. Although the exact mechanism for the propulsion of fuel-driven catalytic nanowire motors is still not fully resolved,[1d] the observed thermally modulated speed appears to primarily reflect heat-induced changes in the kinetics of the fuel redox processes and of the solution viscosity. Indeed, the new data further support the role of the electrochemical processes in the observed motion of catalytic nanowires. The thermal modulation of the movement of artificial nanomotors holds great promise for diverse future applications of functional manmade nanomachines. For example, it would be possible to incorporate multiple heated wires in different locations within a microfabricated channel network for providing an on-demand (spatial and temporal) activation of a nanoscale transport system.

4. Experimental Section

The bisegment nanomotors were prepared by sequential electrodeposition of the Au and Pt segments into a porous alumina membrane template (Catalog no. 6809-6022; Whatman, Maidstone, UK). The branched side of the membrane was initially sputtered with Au. A sacrificial Ag layer of total charge of 2 C was electrodeposited using a commercial Ag plating solution (1025 RTU@4.5 Troy/Gallon; Technic Inc., Anaheim, CA) at a potential of −0.9 V (versus Ag/AgCl (3 M NaCl)), in connection to a Pt wire counter electrode. Subsequently, Au (1.5 C) was electrodeposited at −0.9 V from a Au plating solution (Orotemp 24 RTU RACK; Technic Inc., Anaheim, CA). Pt was then deposited galvanostatically at −2 mA for 50 min from a Pt plating solution (Platinum RTP; Technic Inc). Similarly, magnetic nanomotors were synthesized by introducing a ferromagnetic Ni segment (Au/Ni/Au/Pt). A total charge of 0.5 C of Ni was electrodeposited from a plating solution

© 2009 Wiley-VCH Verlag GmbH & Co. KGaA, Weinheim

[20 g L^{-1} $NiCl_2 \cdot 6H_2O$], 515 g L^{-1} $Ni(H_2NSO_3)_2 \cdot 4H_2O$, and 20 g L^{-1} H_3BO_3 (buffered to pH 3.4)] at −1.0 V (versus Ag/AgCl). The sputtered Au layer and the sacrificial Ag layer were removed simultaneously by rubbing with 35% HNO_3 for ≈3 min to ensure complete Ag dissolution. The membrane was then dissolved in 3 M NaOH for 30 min to completely release nanowires. These nanowires were collected by centrifugation at 10 000 rpm for 5 min and washed repeatedly with nanopure water (18.2 MΩ · cm) until a neutral pH was achieved. All nanowire solutions were stored in nanopure water at room temperature and their speed was tested on the same day of synthesis.

An epoxy well embedded with a Au-coated Pt wire or a Au wire (25-μm-diameter) was prepared on a microscope glass slide to study the effect of temperature on the nanomotor speed (see Supporting Information, Figure S1). While both Au and Pt can be used as materials for the heating wire, the Pt was coated with a dense Au film to suppress spontaneous catalytic decomposition of the fuel. The wire was not stretched straight to provide different source–plane distances in connection to a fine *x-y-z* setting. To measure the distance between the heated wire and the surface of the microscope slide (where the nanomotor movement was monitored), we relied on the micrometer screw on the microscope *x-y-z* stage, calibrated using a short Au wire with a 200-μm diameter. A diluted nanomotor suspension was added to the epoxy well and mixed with a freshly prepared H_2O_2 solution to obtain a final 5% (w/v) concentration. The real time movement of nanomotors was recorded at room temperature and elevated temperatures. Higher temperatures were realized by applying predetermined currents through the heating wire. The heating current was provided by a DC power supply (Agilent E3645A). A logic module (Model "LOGO! 230RC", Siemens AG, Berlin, Germany) was used as a programmable relay to apply the temperature pulses, as was described earlier.[16]

Tracking of nanomotors was performed following the protocol reported earlier.[2] Briefly, an inverted optical microscope (Nikon Instrument Inc., Eclipse TE2000-S) equipped with a 20× objective, a Photometrics CoolSnap CF camera (Roper Scientific, Duluth, GA) and MetaMorph 7.1 software (Molecular Devices, Sunnyvale, CA, USA) were used for capturing movies at a frame rate of 10 frames per second. The depth of the field was very small (≈2 μm), and only the nanomotors on the glass surface were brought into the focal plane. The nanomotor movement was tracked using the Metamorph tracking module and the results were analyzed using OriginPro 7.5 software. The data were smoothed using in-built smoothing functions in OriginPro 7.5.

Tafel plots were used to obtain the mixed potential established at the Au and Pt electrode materials in a 5 wt% H_2O_2 solution. Au and Pt disk electrodes (CH Instruments, Austin, TX) were used as the working electrode in these electrochemical measurements. Cyclic voltammetry of 5 wt% aqueous H_2O_2 (without any electrolyte) was performed using the CH Instrument Model CHI630C at a scan rate of 50 mV s^{-1} and over a potential range of 0.1 to 0.4 V (versus Ag/AgCl), along with Pt wire as a counter electrode. Further details were given earlier.[2]

Estimation of nanomotor temperature: Estimation of the temperature in the plane of the nanomotors was based on earlier simulations of the temperature profile around a heated wire (25-μm-diameter) in vertical[7] and horizontal[6] orientations. We relied on Figure 2 in Reference [6] to estimate the temperature beneath the heated wire. The temperature of the surrounding fluid depends on the distance from the wire surface. Based on the simulations of Beckmann et al.[6] and earlier temperature calibrations for 25-μm Pt[8] and Au[17] wires, we interpolated temperature values for different heating currents between 0 and 900 mA and heat-source distances ranging from 15 to 70 μm. Figure S2 in the Supporting Information displays the 3D plots of the temperature versus heating current versus heat-source distance for the Pt and Au wires. We further assume a negligible change in the bulk temperature (of the entire fluid volume) during our short (1.5–3.0 s) heat pulses and their 10–12 s intermittent cooling periods. This assumption is supported by the following calculation. For example, a heat (Q) of 0.8625 J can be calculated for a 3 s pulse using a 500 mA heating current (I) and a resistance (R) of 1.15 Ω (measured for the Pt wire), based on $Q = t \cdot R \cdot I^2$, where t is the time. Considering a 200 μL bulk volume and the heat capacity of water (4186 J kg^{-1} K^{-1}), we can expect that such a pulse will lead to a maximum increase in the bulk temperature of 1.03 K. On the other hand, heat is removed constantly from the fluid due to thermal conductivity of the glass slide. Hence, we assume that the bulk temperature remains stable during a multipulse experiment over 30 to 60 s periods.

Acknowledgements

This work was supported by the National Science Foundation (Grant Number CHE 0506529). GUF thanks the Deutsche Forschungsgemeinschaft for financial support (Heisenberg fellowship).

[1] a) W. F. Paxton, S. Sundararajan, T. E. Mallouk, A. Sen, *Angew. Chem. Int. Ed.* **2006**, *45*, 5420; b) G. A. Ozin, I. Manners, S. Fournier-Bidoz, A. Arsenault, *Adv. Mater.* **2005**, *17*, 3011; c) W. F. Paxton, A. Sen, T. E. Mallouk, *Chem. Eur. J.* **2005**, *11*, 6462; d) J. Wang, *ACS Nano* **2009**, *3*, 4.
[2] R. Laocharoensuk, J. Burdick, J. Wang, *ACS Nano* **2008**, *2*, 1069.
[3] U. Demirok, R. Laocharoensuk, K. M. Manesh, J. Wang, *Angew. Chem. Int. Ed.* **2008**, *47*, 9349.
[4] T. R. Kline, W. F. Paxton, T. E. Mallouk, A. Sen, *Angew. Chem. Int. Ed.* **2005**, *44*, 744.
[5] a) G. G. Wildgoose, D. Giovanelli, N. S. Lawrence, R. G. Compton, *Electroanalysis* **2004**, *16*, 421; b) P. Gründler, G.-U. Flechsig, *Microchim. Acta* **2006**, *154*, 175; c) P. Gründler, *Curr. Anal. Chem.* **2008**, *4*, 263.
[6] A. Beckmann, B. A. Coles, R. G. Compton, P. Gründler, F. Marken, A. Neudeck, *J. Phys. Chem. B* **2000**, *104*, 764.
[7] K. Frischmuth, P. Visocky, P. Gründler, *Int. J. Eng. Sci.* **1996**, *34*, 523.
[8] P. Gründler, A. Kirbs, T. Zerihun, *Analyst* **1996**, *121*, 1805.
[9] G. Mihajlovic, N. M. Bunet, J. Trbovic, P. Xiong, S. V. Molnar, P. B. Chase, *Appl. Phys. Lett.* **2004**, *85*, 1060.
[10] H. Hess, J. Clemmens, D. Qin, J. Howard, V. Vogel, *Nano Lett.* **2001**, *1*, 235.
[11] T. Zerihun, P. Gründler, *J. Electroanal. Chem.* **1998**, *441*, 57.
[12] S. B. Hall, E. A. Khudaish, A. L. Hart, *Electrochim. Acta* **1999**, *44*, 2455.

 © 2009 Wiley-VCH Verlag GmbH & Co. KGaA, Weinheim

[13] P. Gründler, G.-U. Flechsig, *Electrochim. Acta* **1998**, *43*, 3451.
[14] Y. Wang, R. M. Hernandez, D. J. Bartlett, J. M. Bingham, T. R. Kline, A. Sen, T. E. Mallouk, *Langmuir* **2006**, *22*, 10451.
[15] *Handbook of Chemistry and Physics*, 81st ed. (Ed.: D. R. Lide), CRC Press, Boca Raton, FL **2000**, p. 6.
[16] F. Wachholz, K. Biała, M. Piekarz, G.-U. Flechsig, *Electrochem. Commun.* **2007**, *9*, 2346.
[17] G.-U. Flechsig, O. Korbut, P. Gründler, *Electroanalysis* **2001**, *13*, 786.

Received: January 7, 2009
Revised: February 8, 2009
Published online: March 26, 2009

© 2009 Wiley-VCH Verlag GmbH & Co. KGaA, Weinheim